



## STUDY ON PRESSURE DROP CHARACTERISTICS OF SINGLE PHASE TURBULENT FLOW IN PIPE BEND FOR HIGH REYNOLDS NUMBER

P. Dutta and N. Nandi

Department of Aerospace Engineering and Applied Mechanics, Indian Institute of Engineering Science and Technology, Shibpur, India

E-Mail: [pd.iiest@gmail.com](mailto:pd.iiest@gmail.com)

### ABSTRACT

Pressure drop characteristics of turbulent flow through 90 degree pipe bends are numerically investigated by computational fluid dynamic simulation using k-ε RNG turbulence model with standard wall function. After the validation of present model against existing experimental results, a detailed study has been performed to investigate the pressure distribution and pressure drop characteristics over a wide range of Reynolds number ( $Re = 1 \times 10^5$  to  $10 \times 10^5$ ) and for different curvature ratio ( $R_c/D = 1$  to  $5$ ) to study pressure loss coefficient in terms of Reynolds number and curvature ratio to provide cost effective solutions to design of the pipe bends. A number of important results have been achieved showing the distribution of pressure at different location throughout the bend for different  $Re$  and  $R_c/D$ . Numerical results shows the dependency of pressure distribution and pressure loss coefficient for different Reynolds number and curvature ratio throughout the bend.

**Keywords:** CFD, pipe bend, pressure loss, Reynolds number, single phase, turbulent flow.

### INTRODUCTION

The main characteristics of fluid flow through pipe bends are the presence of adverse pressure gradient developed by the centrifugal force acting on the flow. Due to the presence of centrifugal force and pressure gradient, the fluid moves towards the outer side of the bend and comes back towards the inner side. For a tough bend curvature, this adverse pressure gradient near the inner wall may start the flow separation developing a secondary flow allowing a large increase in pressure loss. This increase of pressure loss experienced in the pipe bends are generated by friction and momentum exchanges appearing from the change of flow direction. Reynolds number, bend curvature ratio and bend angle are the depending factors for this. Therefore, investigations of the flow through bends are of great significance in understanding and improving their performance and minimizing the losses.

The applications of water flows through pipe bends are found in many engineering applications. Some of the excellent reviews bears testimony to this fact [1, 2, 3]. A number of researchers have investigated turbulent flows in a pipe bends by means of theoretical, experiments and numerical methods [4, 5, 6]. Very recent study on turbulent characteristics for single phase flow in large bends provides a new mathematical model for predicting pressure loss by Liwei *et al.*, [7], a numerical and theoretical analysis on pressure characteristics in curved pipe by Zang *et al.*, [8] and detailed study on characteristics of secondary flow and decay of swirl intensity on pipe bends by Kim *et al.*, [9]. Another experimental study of pressure fluctuation [10] and numerical study on pressure drop characteristics and Reynolds number dependency on pipe bend [11] provides very useful data base. Though a number of researchers have already made a significant contribution on the subject, much is yet to be done to present a clear picture of the fundamental characteristics. In this paper the flow characteristics and regularities of distribution in the most

common 90° pipe bend is studied by numerical methods based on computational fluid dynamics. The paper is structured in the following fashion. Section 1 gives a brief idea on the previous research works and motivation for the present work. Section 2 contains the necessary theoretical background. Problem definition with validation is provided in section 3. Section 4 contains the study on various parameters affecting the flow pattern and is followed by summary bulletin of the study under Section 5.

### NUMERICAL METHODOLOGY

#### Governing equations

In the present study, using the segregated implicit solver three dimensional Reynolds averaged Navier Stokes (RANS) equations were solved. The proper selection of a turbulence model is always a crucial job especially when it has a direct application in practical and industrial problem which need a high accuracy modeling. For present study, pressure velocity coupling achieved using SIMPLEC algorithm and the second order scheme was used for the RANS equations calculation. The default under relaxation factors were used to aid convergence for all models.

The governing equations for incompressible fluid flow with constant properties are

$$\frac{\partial \rho}{\partial t} + \nabla \cdot (\rho u) = 0 \quad (1)$$

$$\rho \left( \frac{\partial u}{\partial t} + u \cdot \nabla u \right) = -\nabla p + \mu \nabla^2 u + f \quad (2)$$

Equations (1) and (2) are conservation of mass and momentum, respectively.



### Turbulence model

The main feature of turbulent flow is the fluctuating velocity fields. This fluctuation in velocity fields also be the cause of fluctuation of different transport quantities such as momentum, energy etc. As these fluctuations may be of small scale and high frequency, they are too computationally expensive to simulate directly in practical engineering calculations. The turbulence model needs to be selected based on some considerations, e.g., the physics of the flow, the insight into the capabilities and limitations of turbulence models, the attempt for the specific problem by other researchers, the accuracy needed, the available computational resources, and time.

The k-ε turbulence model is adopted for present study as k-ε turbulence model performs better for single phase flow in pipe bend as suggested by many researchers [9, 12, 13]. In this model, the turbulence kinetic energy ( $k$ ) and the turbulence dissipation rate ( $\epsilon$ ) are solved to determine the coefficient of turbulent viscosity  $\mu_t$ .

Transport equation for  $k$ -epsilon

$$\frac{\partial(pk)}{\partial t} + \frac{\partial(pk u_i)}{\partial x_i} = \frac{\partial}{\partial x_j} \left[ \frac{\mu_t}{\sigma_k} \frac{\partial k}{\partial x_j} \right] + 2\mu_t E_{ij} E_{ij} - \rho \epsilon \quad (3)$$

$$\frac{\partial(p\epsilon)}{\partial t} + \frac{\partial(p\epsilon u_i)}{\partial x_i} = \frac{\partial}{\partial x_j} \left[ \frac{\mu_t}{\sigma_\epsilon} \frac{\partial \epsilon}{\partial x_j} \right] + C_{1\epsilon} \frac{\epsilon}{k} 2\mu_t E_{ij} E_{ij} - C_{2\epsilon} \rho \frac{\epsilon^2}{k} \quad (4)$$

where  $u_i$  represents velocity component in corresponding direction, represents component of rate of deformation, represents eddy viscosity.

The equations (3) and (4) also consist of some adjustable constants, these are as follows

$$C_\mu = 0.09, \sigma_k = 1.00, \sigma_\epsilon = 1.30, C_{1\epsilon} = 1.44, C_{2\epsilon} = 1.92$$

### Boundary conditions

Three types of boundary conditions has been specified for the computational domain. At the inlet, the measured inlet velocity ( $U_m$ ), the turbulent kinetic energy,  $k_{in} = 1.5(I \times U_{in})^2$  where  $I$  is the turbulence intensity, and the

Specific Dissipation Rate  $\epsilon_{in} = \frac{C_\mu k^{3/2}}{(0.3D)}$  are given. The

turbulence intensity has been calculated using the following formula:  $I = 0.16(Re)^{-0.125} \times 100(\%)$  At the wall boundaries, the non-slip conditions have been applied. At the outlet, the gradient of flow variables in the flow direction has been considered as zero.

### PROBLEM DEFINITION

The problem that is considered here is the fluid flow characteristics through two 90° pipe bends having inner diameter of 0.01 m (for present study) and 0.104 m (for validation purpose) for curvature ratio ( $Rc/D$ ) = 1 and 2. The inlet and outlet length of straight pipe in the calculations was set up 20D for both cases to save computational time. The pressure distributions were determined for different Reynolds number ranging from  $1 \times 10^5$  to  $10 \times 10^5$ . The fluid medium was air having density ( $\rho$ ) of 1.2647 kg/m<sup>3</sup> and dynamic viscosity ( $\mu$ ) of  $1.983 \times 10^{-5}$  kg/m-s for validation purpose and water having density ( $\rho$ ) of 998.3 kg/m<sup>3</sup> and dynamic viscosity ( $\mu$ ) of 0.001003 kg/m-s for present study with working temperature of 300 K both cases. For present study three dimensional unstructured mesh was used containing tetrahedron elements, which was optimized via a grid-independence study. The bend geometry and mesh are shown in Figure-1.

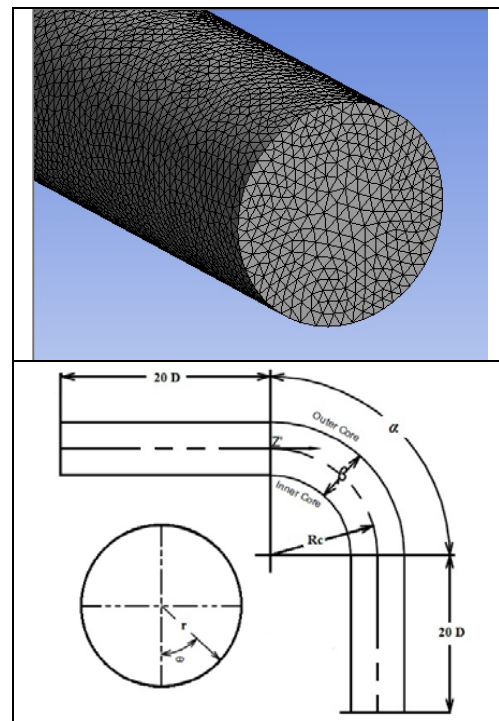


**Figure-1.** Schematic diagram of the bend geometry and present model with computational grid.

### Validation

Distribution of wall static pressure at symmetry plane against the axial angle  $\alpha$ , in the form of the pressure coefficient, obtained by experimental data of Sudo *et al.*, [4] has been compared with numerical result Figure-2 at different sections. For present study, reference pressure has been taken at  $z'/D = -17.6$ . From the validation part it has been seen that present model is in close approximation with the published results, hence this model has been used for further analysis.

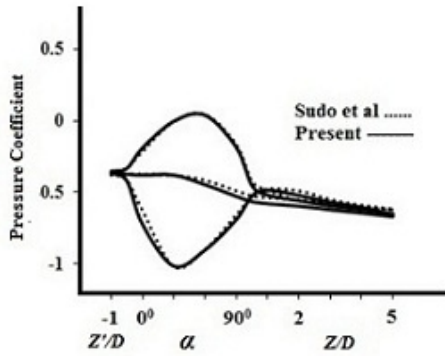


Figure-2. Comparison of pressure coefficient for present turbulent models with experimental.

**RESULTS AND DISCUSSIONS**

The main objective of the present study is to characterize the effect of Reynolds number on single phase turbulent flow in a 90° pipe bend through numerical simulation. The results of the pressure distribution and pressure drop coefficient along the different positions of the bend in central symmetry plane are presented in this section.

**Study on pressure distributions**

The pressure variations along the different positions of the bend in central symmetry plane with different  $Re$  are presented in this section. The minimum value (zero) of  $\beta$  indicates the inner core of the bend and static pressure is normalized with reference pressure taken at  $z/D = -17.6$  as suggested by Sudo *et al.*, [4]. For fixed  $Re (1 \times 10^5)$  and curvature ratio  $Rc/D = 1$ , Figure-3 shows the variation of the dimensionless pressure with normalized bend cross-sectional length  $\beta$  for different axial angle  $\alpha$ . It can be seen that the maximum pressure is observed at outer core and minimum at the inner core as expected. This happens due to the presence of centrifugal force.

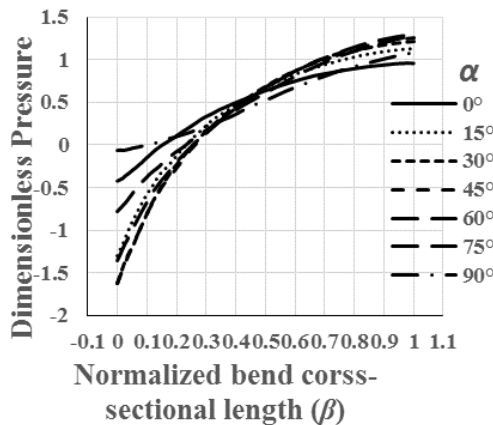


Figure-3. Pressure distribution along the normalized bend cross-sectional length ( $\beta$ ).

To evaluate the dependency of pressure on Reynolds number, Figure-4 shows dimensionless pressure with Reynolds number through the bend. It can be seen from Figure-4 that, the dimensionless pressure has little change with the Reynolds number in the inner and outer core of the bend, and it tends to a constant value when the Reynolds number becomes increasingly larger  $Re \geq 3 \times 10^5$ . Pressure in the middle core is almost constant throughout the bend. This observation is also consistent with Dutta *et al.*, [11].

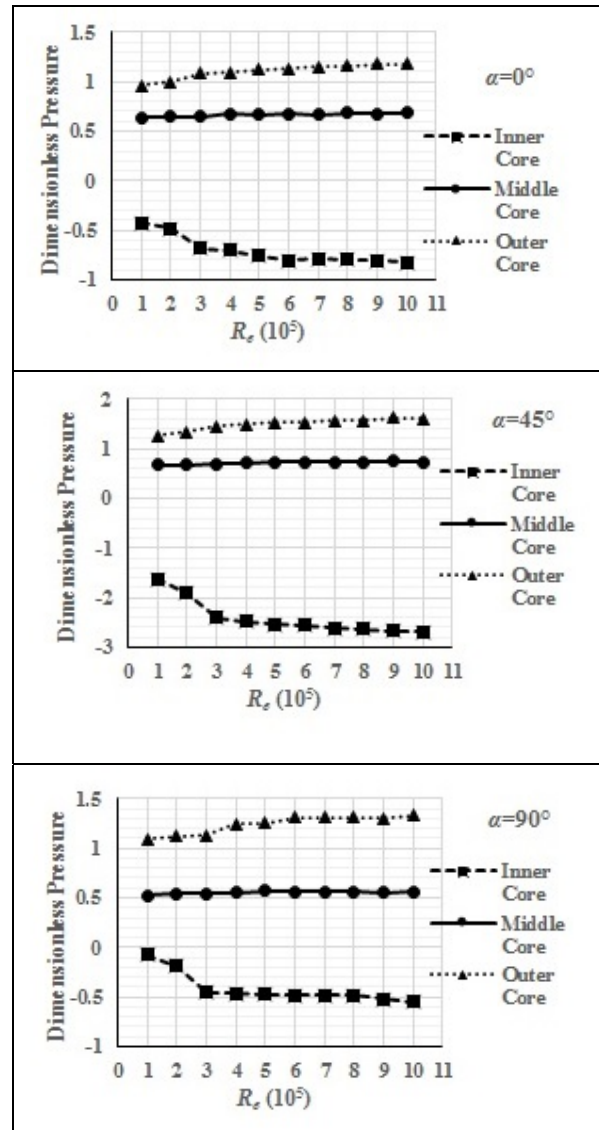


Figure-4. Variation of dimensionless pressure with Reynolds number.

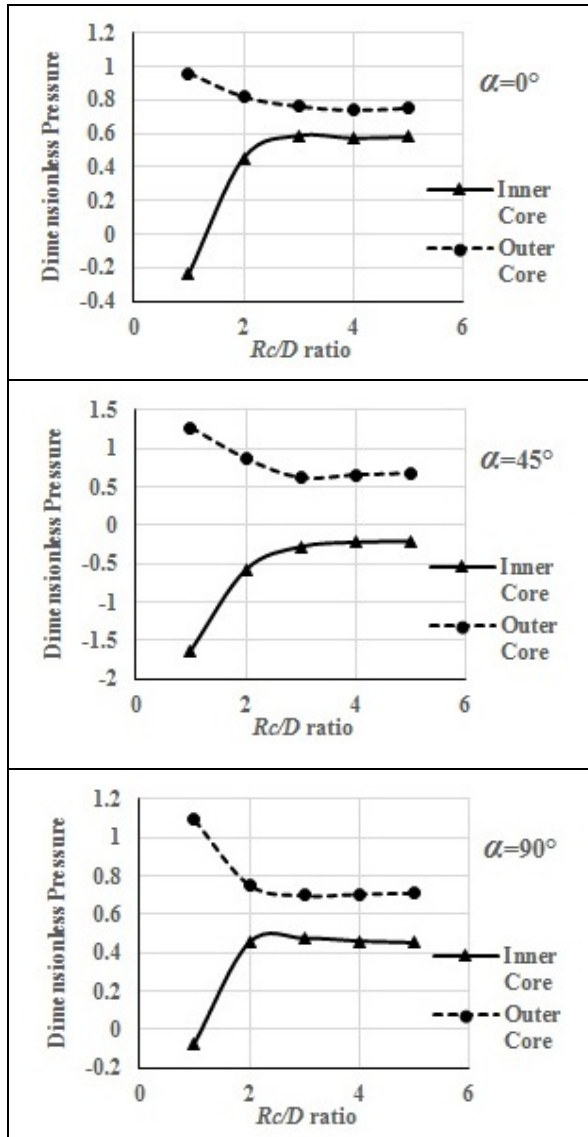


Figure-5. Variation of dimensionless pressure with curvature ratio.

Figure-5 shows the dimensionless pressure changes with the change of bend curvature ratio  $Rc/D$ , keeping Reynolds number unchanged  $Re (1 \times 10^5)$ . It can be seen from Figure-5, (1) the dimensionless pressure on outer core decreases with the curvature ratio increases, which tends to a constant value when  $Rc/D \geq 3$ ; (2) the dimensionless pressure on the inner core increases with  $Rc/D$  increases, which tends to a constant value when  $Rc/D \geq 3$ . This observation is also consistent with Zang *et al.*, [8].

### The pressure drop characteristics

Another attempt was done to characterize the pressure drop characteristics in the bend for different curvature ratios with different Reynolds numbers. The variation of normalized mass averaged total pressure loss

coefficients based on the mass average pressure at different sections of the bend having fixed curvature ratio are shown in Figure-6. It was calculated based on the static pressure difference between the succeeding and reference sections. The pressure loss coefficient  $k_p$  can be defined as

$$k_p = \frac{\nabla p}{0.5 \rho U_{in}^2} \quad (5)$$

where  $\nabla p$  is the total pressure loss across the bend.

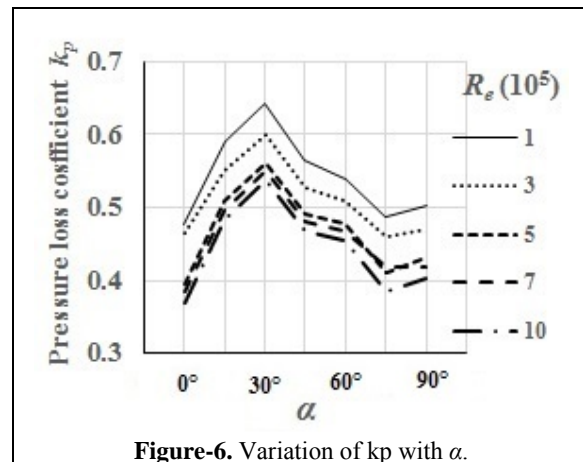


Figure-6. Variation of  $k_p$  with  $\alpha$ .

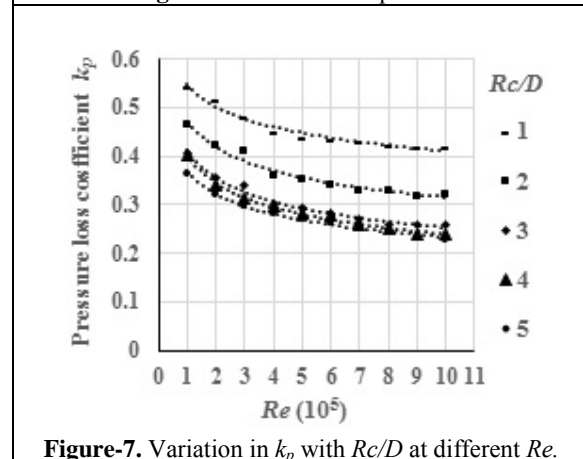


Figure-7. Variation in  $k_p$  with  $Rc/D$  at different  $Re$ .

From the Figure-6 it has been observed that maximum pressure loss coefficient applies at  $\alpha = 30^\circ$ , this is mainly due to the development of secondary flow and magnified swirl intensity of secondary flow and as  $Re$  increases, pressure loss coefficient  $k_p$  becomes lower and almost same for higher  $Re$  due to higher velocity heads.

Figure-7 shows the dependency of average pressure loss coefficient on Reynolds number and curvature ratio. It is observed that pressure loss coefficient has a weak dependency on high Reynolds number. As Reynolds number increases, the rapid change of pressure increase the both separation and friction effects, despite of lower pressure loss coefficient due to higher velocity head.





## CONCLUSIONS

Turbulent flow of single phase incompressible fluid through 90° pipe bend has been simulated numerically using  $k-\varepsilon$  RNG turbulence model in the present study. The validation of 3D models used for present study with experiments reported by Sudo *et al.*, [4] indicates a good agreement. From the present study, it can be concluded that the normalized pressure has a little change with Reynolds number and it tends to almost constant value for high Reynolds number ( $Re \geq 3 \times 10^5$ ). Normalized pressure on the inner core increases with curvature ratio and on the outer core decreases with curvature ratio, and these tend constant when curvature ratio. Pressure difference between inner and outer core of the bend decreases as curvature ratio increases and

become a constant value for bend with high curvature ratio. Due to the secondary flow, maximum pressure loss coefficient applies at  $\alpha=30^\circ$  then decreases. Bends having a small curvature ratio, which adds the significant pressure loss, causes a rapid rise in pressure loss coefficient  $k_p$ , and this tends to constant for higher curvature ratio. The above conclusions refer specially for present study range. However, additional studies are necessary to provide a correlation between pressure loss coefficient and the bend curvature ratio.

## Notation

The following symbols are used in this paper:

$Re$	=	Reynolds number	$\mu_t$	=	eddy viscosity
$D$	=	bend diameter	$U_{in}$	=	inlet velocity
$Rc$	=	radius of bend curvature	$\vec{U}$	=	vector of the flow velocity
$\alpha$	=	bend axial angle, ( $0^\circ \leq \alpha \leq 90^\circ$ )	$u_i$	=	velocity component
$\beta$	=	bed cross-sectional length,	$E_{ij}$	=	component of rate of deformation
$r, \theta, z$	=	radial, circumferential, axial	$k_p$	=	pressure loss coefficient
coordinates			$I$	=	turbulence intensity
$z'$	=	distance along pipe axis	$\varepsilon$	=	specific dissipation rate
$\mu$	=	dynamic viscosity of fluid	$k$	=	turbulent kinetic energy
$\rho$	=	density of fluid			

## ACKNOWLEDGEMENT

Part of this paper has been already presented in International Symposium on Aspects of Mechanical Engineering and Technology for Industry (AMETI 2014), NERIST- Arunachal Pradesh, INDIA, 6-8 December 2014.

## REFERENCES

- [1] Spedding P. L., Benard, E. and McNally, G. M. 2004. Fluid flow through 90 degree bends. Developments in Chemical Engineering and Mineral Processing. 12(1-2): 107-128.
- [2] Naphon, P. and Wongwises, S. 2006. A review of flow and heat transfer characteristics in curved tubes. Renewable and sustainable energy reviews. 10(5): 463-490.
- [3] Crawford, N., Spence, S., Simpson, A. and Cunningham, G. 2009. A numerical investigation of the flow structures and losses for turbulent flow in 90° elbow bends, Proceedings of the Institution of Mechanical Engineers, Part E: Journal of Process Mechanical Engineering. 223(1): 27-44.
- [4] Sudo, K., Sumida, M. and Hibara, H. 1998. Experimental investigation on turbulent flow in a circular-sectioned 90-degree bend, Experiments in Fluids. 25(1): 42-49.
- [5] Sakakibara, J. and Machida, N. 2012. Measurement of turbulent flow upstream and downstream of a circular pipe bend, Physics of Fluids (1994-present), 24(4): 041702
- [6] Kalpakli, A., Örlü, R. and Alfredsson P. H. 2012. Dean vortices in turbulent flows: rocking or rolling, Journal of Visualization. 15(1): 37-38.
- [7] Wang, L., Gao, D. and Zhang, Y. 2012. Numerical simulation of turbulent flow of hydraulic oil through 90° circular-sectional bend, Chinese Journal of Mechanical Engineering. 25(5): 905-910.
- [8] Zhang, H., Zhang, X., Sun, H., Chen, M., Lu, X., Wang, Y. and Liu, X. 2013. Pressure of Newtonian fluid flow through curved pipes and elbows, Journal of Thermal Science. 22(4): 372-376.
- [9] Kim, J., Yadav, M. and Kim, S. 2014. Characteristics of secondary flow induced by 90-degree elbow in turbulent pipe flow, Engineering Applications of Computational Fluid Mechanics. 8(2): 229-239.
- [10] Shiraishi, T., Watakabe, H., Sago, H., and Yamano, H. 2009. Pressure fluctuation characteristics of the short-radius elbow pipe for FBR in the post critical



- Reynolds regime. *Journal of Fluid Science and Technology*. 4(2): 430-441.
- [11] Dutta, P., Banerjee, S., Santra, A., and Nandi, N. 2014. Numerical Study on Pressure Drop Characteristics of Turbulent Flow in Pipe Bend. *Proceedings of the International Symposium on Aspects of Mechanical Engineering and Technology for Industry (AMETI 2014), NERIST - Arunachal Pradesh - India*. 1: 381-386.
- [12] Homicz, G. F. 2004. *Computational Fluid Dynamic Simulations of Pipe Elbow Flow*. United States, Department of Energy.
- [13] Rahimzadeh, H., Maghsoodi, R., Sarkardeh, H. and Tavakkol, S. 2012. Simulating flow over circular spillways by using different turbulence models. *Engineering Applications of Computational Fluid Mechanics*. 6(1): 100-109.